

## **Chapter – 2**

### **Nuclear Modular and Transport Codes**

- 2.1 Introduction**
  - 2.2 Nuclear Reaction Models**
    - 2.2.1 Compound nucleus mechanism**
    - 2.2.2 Direct reaction**
    - 2.2.3 Pre-equilibrium**
    - 2.2.4 Optical model**
    - 2.2.5 Nuclear level density**
      - 2.2.5.1 Composite Gilbert-Cameron model**
      - 2.2.5.2 The Back-shifted Fermi gas Model**
      - 2.2.5.3 The Generalized Superfluid Model**
      - 2.2.5.4 The Enhanced Generalized Superfluid Model**
      - 2.2.5.5 Microscopic level densities**
  - 2.3 TALYS**
  - 2.4 EMPIRE**
  - 2.5 Monte Carlo N-Particle Code (MCNP)**
  - 2.6 Summary**
  - References**
-

## 2.1 Introduction

The importance of the nuclear data in the frame of reactor development has been discussed in the previous chapter. In order to have a complete set of nuclear data, there should be complete measurements of all reaction channels on all targets and with all projectile energies. This cannot be possible to achieve with experiments only. It is not feasible to make all the isotopic targets, which may itself be radioactive and may not be available with proper physical states. In order to theoretically explain these experimental results, it is required to have a set of well-designed nuclear reaction models. There are several nuclear reaction models that have been provided by different authors. The worldwide nuclear community has taken them as a base and using the computer programming, they have made different nuclear codes, which can predict the nuclear data. The codes are of two types: (1) Nuclear modular codes, and (2) Nuclear transport codes. The nuclear modular codes can predict the nuclear data such as reaction cross section, the angular distribution of outgoing particles etc., i.e., they can generate the basic nuclear data, and by using nuclear data one can make nuclear data library. The nuclear transport codes use this data library to transport the particle of interest and predict answers of the certain problems/requirements such as particle flux, reaction rates etc. These codes are very important as they can predict the data interpolation, extrapolation for all kinds of targets, particles, and energies. It can delimit the experimental limitations. But it is also necessary to validate the codes by comparison of code predicted data with experimental data.

In the present thesis, the nuclear modular codes TALYS and EMPIRE, and nuclear transport code MCNP have been used. The different reaction models are discussed briefly in the following sections.

## 2.2 Nuclear Reaction Models

There are several nuclear reaction models that have been developed by several researchers in the past, in order to explain the experimental results. The agreement with the experimental data shows the reliability of the nuclear models as well as it also identifies the limits of the model. It is of great interest to make more and more accurate nuclear reaction models to achieve highly reliable data. Basically, there are three nuclear reaction mechanisms as per the energy range of the incident particles,

which have been incorporated in various reaction models: (1) compound nucleus, (2) direct reaction, and (3) pre-equilibrium reaction mechanisms. Overall nuclear reaction mechanisms are shown in **FIG 2.1**. The role of these reaction mechanisms in reaction products with respect to the energy of the projectile is shown in **FIG 2.2**.

## 2.2.1 Compound nucleus mechanism

This reaction mechanism was explained by Bohr (1936) [1]. When a low energy particle/nucleon is incident on a target nucleus and enters into it, it distributes all its kinetic energy among all the nucleons of the target nucleus. Hence, the nucleus, which was in the ground state, is now having some excess amount of energy, and it is now in the excited state. This state having an equilibrium with a very small mean lifetime of the order of  $\sim 10^{-16}$  s. It has no memory of its formation. It then decays and emits an ejectile and a residue. Suppose a nucleon 'a' incident on a target 'A', and the compound nucleus 'A\*' has been formed before it gives the products, 'b' and 'B', can be written as,

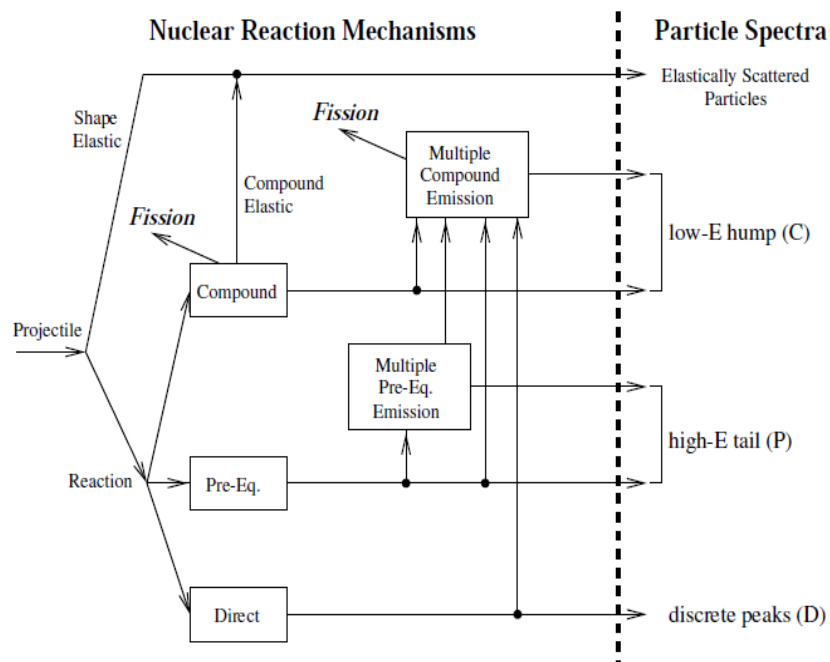


**FIG 2.1** Nuclear reaction mechanisms

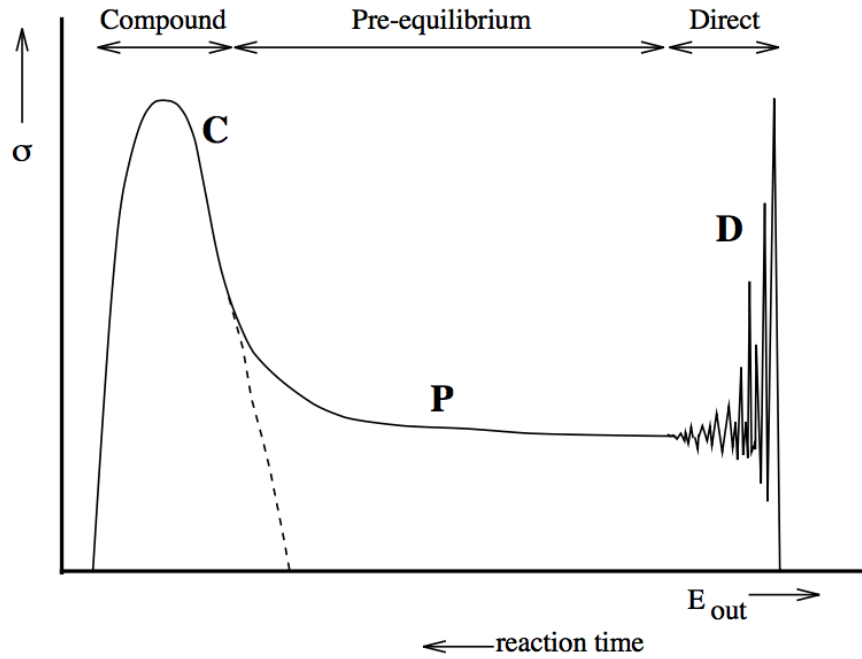


**FIG 2.2** Outgoing particle spectra; the role of compound nucleus (C), pre-equilibrium (P) and direct reaction (D) mechanism with respect to incident particle energy

The compound nucleus mechanism has been incorporated in the Weisskopf – Ewing and Hauser-Feshbach models [2,3]. The reaction mechanism can be divided into two stages; in the first stage the formation and in the second stage the decay of compound nucleus takes place. The energy lost by the projectile in the target nucleus makes the compound nucleus, which is in the excited state. In the second stage, the excess amount of energy releases by the emission of electromagnetic radiation or an ejectile particle. The decay of the compound nucleus is shown in **FIG 2.3**.

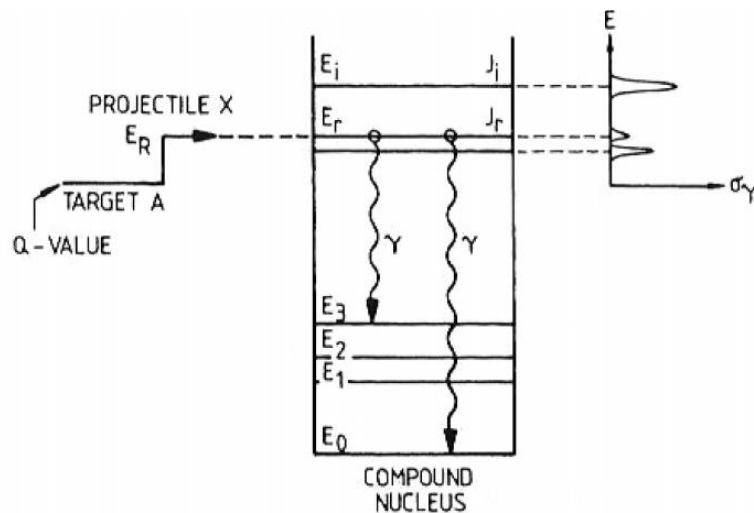


**FIG 2.3** Decay of compound nucleus

### 2.2.2 Direct Reaction

The direct reaction takes place in the least time  $\sim 10^{-22}$  s, which is almost equal to a particle to pass through a nucleus. In this mechanism, an incident particle may pick a nucleon or nucleons from the target nucleus or it may lose its constituent particles in the target. The former reaction is called pick up while the later one is called stripping reaction. Another possibility is inelastic scattering in which, a particle just interact and loses or gains some amount of energy and ejects a particle. This reaction is probable for the particle with higher energy ( $>10\text{MeV}$ ). In the direct reaction mechanism, the associated angular distributions are strongly peaked in the forward direction and have oscillatory behavior. It is possible to deduce the spin and parity of the residue from this oscillatory shape of the spectrum. The Distorted Wave Born Approximation (DWBA) or couple channeled approach can be helpful to understand the direct reaction mechanism. Here in this direct reaction mechanism, the target nucleus does not go into the compound nucleus stage, i.e., there is no transient equilibrium stage in the reaction.

The examples of direct reactions are as given below.

Stripping reaction:  $A(d, n)B$ ,  $A(d, p)C$ , etc.

Pick up reaction:  $X(n, d)Y$  or  $X(n, t)Z$ , etc.

Inelastic scattering:  $A(n, n')A$

### 2.2.3 Pre-equilibrium Reaction

In compound nucleus mechanism a nucleus goes in a transient equilibrium stage and then it decays, whereas, in the direct reaction mechanism, there is no equilibrium. In the process, before the nucleus goes to complete statistical equilibrium it decays to reaction products and such reactions are called the pre-equilibrium process. In the 1950s, the experimental data were found which cannot be completely explained by the compound nucleus or direct reaction mechanism. These data were in the moderated energy range. It suggests that there may be another kind of mechanism lies in between of these two mechanisms i.e., the pre-equilibrium. This mechanism is important from 10 MeV to  $\sim 200$  MeV. The mechanism suggests that the nucleus goes to series of excited state and creates complex energy structure in the nucleus, but before it goes to a statistical stable stage with a particular angular momentum it

decays. This mechanism can be explained with two semi classical models from Griffin (1966) and Kalbach (1973), which are called exciton model and hybrid model respectively [4,5].

According to exciton model, once the projectile enters the target nucleus, the system gets excited with series of stages and different angular momenta. Before it goes to the final stage of equilibrium, it emits the ejectile (PE particles) and residue. The energy transferred by the projectile in the target nucleus decides the complexity of the stage, which can be estimated with the number of particles and holes excited. These excited particles and holes are called excitons. By solving the dynamical equations of these excitons one can calculate the resultant stage and products from the reaction. This mechanism can be explained by FIG 2.4. The  $E_F$  is the Fermi energy of the system.

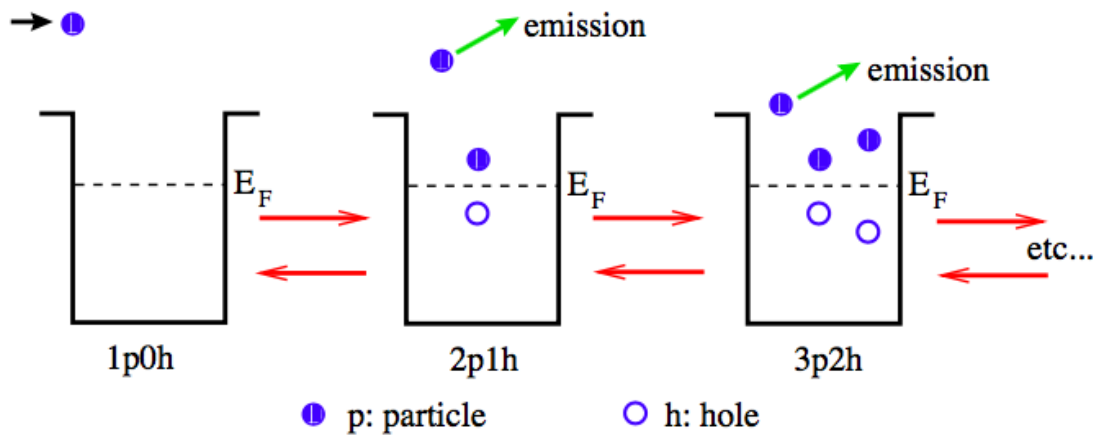


**FIG 2.4** Pre-equilibrium mechanism as explained in the exciton model

From FIG 2.4, it can be understood that an incident particle  $p$ , interacts with another particle below the Fermi sea, and excites it to make  $2p1h$  ( $h$  = hole) stage. In next stage, it reaches to stage  $3p2h$  and so on. These stages are reversible. Before it goes to a stable stage any one stage can give the reaction products. In addition to this exciton model, there are many other pre-equilibrium models that have been proposed to explain this reaction mechanism. A quantum approach, which is used to overcome the deficiency of these models are the multi-step compound model (MSC) by Nishioka *et al.*, (1986) [6] and multi-step direct model (MSD) by Nishioka *et al.*, (1988) [7]. In MSC, all the particles are in the bound state, whereas in the MSD at least one particle is necessary to be in a continuum or above binding energy. Also, the MSC shows emission of particles is symmetric around  $90^\circ$ , whereas in MSD it is forward peaked.

The MSD uses the DWBA approach. For the data prediction, both the MSC and MSD should be applied together.

### 2.2.4 Optical Model

When a nuclear reaction takes place, the two nuclei combine together, and in this system, a single nucleon is in the field created by all the remaining nucleons. If we have N number of nucleons in a system then N number of Schrödinger's equations are required to represent the system. It is necessary to have the appropriate form of potential in order to solve the equations. In the optical model, this potential is considered complex, which has a real part as well as an imaginary part. The interaction between the incident particle and the nucleus is considered as an optical phenomenon. As an electromagnetic wave enters one media to another media, it may get refracted and when some obstacle is in the path it may get diffracted. In the same manner, the incident particle wave is diffracted by the nucleus. Hence the overall potential  $V(r)$  contains a real part representing the diffraction phenomenon and imaginary part representing the refraction part. The potential is represented by the following equation, with real part  $U(r)$ , and imaginary part  $W(r)$ .

$$V(r) = U(r) + jW(r)$$

The model was proposed by Bethe (1937) [8], which was explored by Feshbach *et al.* (1954) [3] in order to apply on neutron induced nuclear reactions. The Optical model is effective and reliable in explanation of most of the experimental data. This model has been modified as per the requirements from time to time.

### 2.2.5 Nuclear level density

The quantum mechanics says that the energy is quantized which generates the energy states. The energy states per unit energy interval are called nuclear level density. This parameter plays a crucial role in the nuclear reaction mechanism. In 1936, Bethe had done important work in the field of nuclear level density. If the density is more, then the spacing between the energy states is small. Ideally, if it is infinity, then the state will be a continuum. This parameter has given great importance to the development of nuclear modular codes. There are different level density models given in TALYS and EMPIRE codes [9, 10]. In present work, the effectiveness of these models has been tested and presented in Chapters – 4-5. The brief idea about each model used for level

density is given here. In the latest version of TALYS – 1.8, there are total six level density models are given, whereas in EMPIRE, in recent version there are five models are included.

The basic formula of the level density was given by Bethe as the expression below.

$$\Delta E^{ex} = \frac{1}{\rho(E^{ex})}$$

Where,  $\Delta E^{ex}$  is the energy interval and  $\rho(E^{ex})$  is the level density.

It suggests that a nucleus can be considered as a gas of nucleons, and a nucleon can occupy a particular energy level depending on the temperature of the nucleus. Hence, the nuclear level density can be written as,

$$\rho(E^{ex}) = ce^{2\sqrt{aE^{ex}}}$$

Where  $c$  is proportionality constant,  $a$  is the level density parameter and  $E^{ex}$  is the excitation energy of the compound nucleus. The parameter  $a$  is adjusted in such way that the evaluated data agrees with the experimental data. This model is also considered as constant temperature model. The other models of the level density are modification of this basic concept.

### 2.2.5.1 Composite Gilbert-Cameron model

The constant temperature level density formula was modified by Gilbert Cameron in 1965 as given below.

$$\rho_T(E) = \frac{1}{T} \exp \left[ \frac{E - \Delta - E_0}{T} \right]$$

Where  $T$  is the temperature,  $E$  is the excitation energy,  $\Delta$  is the pairing energy,  $E_0$  is the adjustable energy shift. And for the case where the excitation energy  $E >$  matching point energy  $U_x$ , the Fermi gas formula is used.

$$\rho_f(U) = \frac{\exp(2\sqrt{aU})}{12\sqrt{2}\sigma^2(U)a^{\frac{1}{4}}U^{\frac{5}{4}}}$$

Where,  $\sigma^2$  is spin cut of parameter,  $a$  the level density parameter is given by,

$$a(U) = \tilde{a} \left( 1 + \delta W \frac{1 - \exp(-\gamma U)}{U} \right)$$

Where,  $\tilde{a}$  is the asymptotic level density parameter,  $\delta W$  is the shell correction energy and  $\gamma$  is the damping parameter. The asymptotic level density parameter is given by,

$$\tilde{a} = \alpha A + \beta A^{\frac{2}{3}}$$



Where  $A$  is the mass number,  $\alpha$  and  $\beta$  are the global parameters.

### 2.2.5.2 The Back-shifted Fermi Gas Model

In this model, the pairing energy is treated as an adjustable parameter [11]. The Fermi gas expression is used to reach up to 0 MeV. The total density is given as,

$$\rho_F^{tot}(E_x) = \frac{1}{\sqrt{2\pi}\sigma} \frac{\sqrt{\pi} \exp(2\sqrt{aU})}{12 \frac{a^{1/4} U^{5/4}}{a^{1/4} U^{5/4}}}$$

And the level density is,

$$\rho_F(E_x, J, \pi) = \frac{1}{2} \frac{2J+1}{2\sqrt{2\pi}\sigma^3} \exp\left[\frac{\left(J + \frac{1}{2}\right)^2}{2\sigma^2}\right] \frac{\sqrt{\pi} \exp(2\sqrt{aU})}{12 \frac{a^{1/4} U^{5/4}}{a^{1/4} U^{5/4}}}$$

### 2.2.5.3 The Generalized Superfluid Model

The generalized superfluid model (GSM) is based on the theory of Bardeen-Cooper-Schrieffer on superconducting nature. The phenomenological model is characterized by a phase transition of superfluid behavior at low energy [12,13], where the level density is strongly influenced by pairing energy term. The GSM model distinguishes between a low and high energy region. An additional shift of the excitation energy  $\delta_{shift}$  is introduced in the GSM was introduced to the enhancement of the level density parameter [13].

$$U = E_x + n\Delta_o + \delta_{shift}$$

Where  $\Delta_o = 12/\sqrt{A}$  and  $n = 0, 1$  and  $2$  for even-even, odd-A and odd-odd nuclei, respectively.

$$a(U, Z, A) = \begin{cases} \tilde{a}(A) \left(1 + \delta E_0 \frac{f(U^*)}{U^*}\right), & U \geq U_{cr} \\ a_{cr}(U_{cr}, Z, A), & U \leq U_{cr} \end{cases}$$

Where  $U_{cr}$  is the condensation energy is subtracted from the effective excitation energy. A further detail of the model is given in TALYS and EMPIRE manual [9,10].

#### 2.2.5.4 The Enhanced Generalized Superfluid Model

The Enhanced Generalized Superfluid Model (EGSM) also uses the superfluid model below the excitation energy and above it the Fermi gas model as similar to GSM. It includes the enhancement of spin distribution contribution in Fermi gas model which is different from the GSM [14]. The enhancement of the level density for the evaluation is achieved from the non-adiabatic form of nuclear rotation. Hence it considers the shape of the nucleus in the dynamical situation. This deformation enters level densities formulas through moments of inertia and through the level density parameter that increases with increase in the surface of the nucleus. In the parameterization of ESGM, the role of the nuclear surface term and linear dependency on asymptotic  $\tilde{a}$  vanished, and covers collective enhancement. ESGM global systematics does not account for discrete levels.

#### 2.2.5.5 Microscopic level densities

There are different microscopic methods available to calculate the level densities. The GSM approach has been used in the microscopic superfluid model to calculate the level density and other parameters of the excited nucleus. It considers realistic single particle level schemes [15]. The codes use this approach in the collective mode to generate the level density for the reaction data prediction. There are two main microscopic level density models used in the development of the codes. For RIPL data library, S. Goriely has calculated the level densities using the Hartree-Fock calculations [15] for excitation energies up to 150 MeV and for spin values up to  $I = 30$ . Including this new energy, spin and parity dependent nuclear level densities based on the microscopic combinatorial model have been proposed by Hilaire and Goriely [16]. This model includes the intrinsic state density and collective enhancement. The calculations make coherent use of nuclear structure properties determined within the deformed Skyrme-Hartree-Fock-Bogolyubov framework [17]. The temperature-dependent Hartree-Fock-Bogolyubov calculations using the Gogny force is also included in the recent versions of the codes.

## 2.3 TALYS

The TALYS is a nuclear modular code, which was developed by A. J. Koning, S. Hilaire and M.C. Duijvestijn [9], which is a complex code using the different nuclear reaction models in a computer program. It is a Linux based program and can be installed on Linux and Mac OS with FORTRAN or c programming. The first version of TALYS – 1.0 was released in 2007. Time to time it was modified and next versions TALYS – 1.2, 1.4, 1.6, and latest TALYS – 1.8 (2016) were released. The code was developed to do a simulation on nuclear reactions induced by neutrons, photons, protons, deuterons, tritons,  $^3\text{He}$ - and alpha-particles, in the energy range 1 keV – 200 MeV and for target nuclides of mass 12 and heavier [9].

In the evaluation of nuclear reaction data it uses different nuclear models which are written in the subroutines of the main code, and the parameters necessary for the evaluations are taken from the Reference Input Parameter data Library – 3 (RIPL) developed by IAEA [18]. The basic requirements of a TALYS input file are projectile, element, mass, and energy. One can run input with default parameters or with multiple options and parameters provided in the TALYS manual [9]. In the output, one can get all possible reaction channel nuclear data such as reaction cross sections, angular distribution, the cross section from different excitation levels, etc. It uses different level density models with *ldmodel* parameters. In TALYS – 1.8 there are six different combinations of nuclear level densities has been used [9].

*ldmodel* 1: Constant temperature + Fermi gas model

*ldmodel* 2: Back-shifted Fermi gas model

*ldmodel* 3: Generalised superfluid model

*ldmodel* 4: Microscopic level densities (Skyrme force) from Goriely's tables

*ldmodel* 5: Microscopic level densities (Skyrme force) from Hilaire's combinatorial tables

*ldmodel* 6: Microscopic level densities (temperature dependent HFB, Gogny force) from Hilaire's combinatorial tables

In present thesis work, the effect due to this parameter on selected nuclear reactions has been investigated. In the case of default input parameters, it uses *ldmodel* 1.

## 2.4 EMPIRE

EMPIRE (-3.2.2) Malta is a modular system for nuclear reaction calculations and nuclear data evaluation [10]. It can evaluate data for photons, nucleons, deuterons, tritons, helions ( $^3\text{He}$ ),  $\alpha$ 's, and light or heavy ions. It takes range from few keV to several hundred MeV. It considers the major nuclear reaction models: Optical model, DWBA, Couple channels, MSD, MSC, exciton model (PCROSS) hybrid Monte Carlo simulation (DDHMS), and the full featured Hauser-Feshbach model including width fluctuations and the optical model for fission [10]. It uses CCFUS for heavy ion induced fusion. EMPIRE also uses the parameters from RIPL – 3 data library [18]. It is also Unix/Linux based code, but Windows version is also available. The first version of EMPIRE was released in 1980. The latest version of EMPIRE code is EMPIRE – 3.2.2 Malta. This version included combinatorial calculations of particle-hole level densities. In present thesis work, the following level density models were used for the investigation. It can be defined with LEVDEN mnemonic.

LEVDEN

- = 0 EMPIRE-specific level densities, adjusted to RIPL-3 experimental Dobs and to discrete levels (default),
- = 1 Generalized Superfluid Model (GSM, Ignatyuk et al), adjusted to RIPL experimental Dobs and to discrete levels,
- = 2 Gilbert-Cameron level densities (parameterized by Ijnov et al), adjusted to RIPL experimental Dobs and to discrete levels,
- = 3 RIPL-3 microscopic HFB level densities, parity dependent NLD,
- = 4 Gilbert and Cameron NLD.

This parameter was changed to study the effect of on the magnitude and shape of nuclear reaction cross sections with respect to energy. Further detail of several parameters used for the data evaluation is discussed in EMPIRE manual.

## 2.5 Monte Carlo N-Particle Code (MCNP)

The Monte Carlo N-Particle – MCNP code was developed to transport the particles through the materials using Monte Carlo method. It was developed and maintained by Los Alamos National Laboratory [19-21]. It can transport neutron, proton, electron, photon and many other particles. It can transport in a single particle mode as well as in multiple particle transport mode. It is a worldwide recognized code for particle transport. It is useful in simulation for shielding design, radiation protection and dosimetry, medical physics, nuclear critical safety, detector design and analysis, accelerator and target design, reactor design parameters, detector signal generation etc. [20, 21].

The MCNP code gives facility to user to make a 3d model of the problem geometry. It has a particular input file consisting the description of the problem, which is described by different mnemonics known as CARDS. There are mainly three blocks: 1. Cell cards, 2. Surface cards and 3. Data cards. With these cards, the user has to define the problem geometry, materials to be used in the geometrical shapes, mode of transport, source description and the detectors. To perform these calculations, MCNP needs cross section data library. The inbuilt data library is ENDF-B/VI for neutron transport [20]. Further, there are different libraries such as IRDF-2002, FENDL-2.1, ENDF upgraded versions, and many other data libraries can be used to perform the calculations. For different particles different data libraries are available. While running the program it calls these libraries for the particle transport. A brief idea of an MCNP input file has been given here.

Input file:

The input file for MCNP is a text file containing geometry specification and data information using the above three parts in it. All the three parts are necessary to run a program.

1. Surface Cards;

Surface cards are imaginary surfaces defined by these cards, e.g. plane, a spherical surface, cylindrical surfaces etc. These imaginary surfaces can be used to make the volume shapes by Boolean operations. The Boolean operations such as AND, OR, NOT are used to make shapes. AND operation is specified by space i.e., surface 1 and surface 2, the AND operation is specified by 1 2. The OR operation is specified by ‘.’ symbol in between

surfaces, e.g., 1:2. The NOT operation is specified by ‘#’ symbol, e.g., #1. All surfaces are represented using the Cartesian coordinate system as an  $f(x,y,z) = 0$ . For example, a spherical surface with the origin as a center and R as a radius is given by  $x^2 + y^2 + z^2 - R^2 = 0$ . Its surface card is given as

1 S 0 0 0 10

\$ center is origin, radius = 10cm

**or** 1 SO 10

With this card, the software will create an imaginary sphere with the center as origin and 10 cm radius. The number of this surface denoted is 1. Multiple surfaces with the Boolean operation can make shapes termed out as cells. More details of this card are available in Volume – 1 of manual of the code [14].

## 2. Cell Cards:

The cell cards are used to make three-dimensional geometrical shapes using the surface cards. One can make the experimental setup design in MCNP using this cards. These cells must be filled with the appropriate materials, which can be defined by using the material card.

For example, if a cube box is used to shield a radiation source, the box can be defined with six surfaces and Boolean logic. In a cell definition, the first number is a cell identity, secondly is for the material identification number. It may be zero (0) if no material (void) is selected, or a number followed by density. If density is in g/cc then negative sign (–) is used before it, and if it is an atom density then positive sign (+) is used. After that, the surface Boolean operations are used. At the end, the important card is used, which is defined by the particles, for neutron “n”, photon “p”, etc. and its weightage.

Surface cards:

1 px -10

2 px 10

3 py -10

4 py 10

5 pz -10

6 pz 10

Cell Cards:

Cell no	material	Boolean of surfaces	particle for transport
1	0	1 -2 3 -4 5 -6	imp:n=1

or

1	2 -1.0	1 -2 3 -4 5 -6	imp:n=1
---	--------	----------------	---------

### 3. Data Cards:

The data cards are in general contain a large number of information about source description, material description, detector description and run control cards.

The source is defined by SDEF (Source DEFinition) card, which contains information about source position, particle type (n/p/e), particle energy, etc., which are necessary for complete source description. The position, energy, and dimension of the source can be written in terms of distribution if it is required. The details can be found in MCNP manual volume – II [22, 23].

Another card is a material card, which specifies the isotopic composition of the material used in the problem. It is specified by the “m” letter, followed by ZZZAAA.xx format, where ZZZ is for isotope number and AAA is for atomic mass number of the isotope. The .xx is for the data file extension that may be .60c, .21d, etc., likewise. The “c” stands for continuous and “d” for discrete data points in the data library. For e.g., water can be specified with two elements: H and O. Its atomic mass is 18 g, which is from 2 H atom and 1 O atom. The fraction of weight contribution from 18 g of H is  $2 \times \text{H mass} \div 18 \text{ g}$  and from O is  $1 \times \text{O mass} \div 18 \text{ g}$ . The values are 0.1112 and 0.8888 respectively. So m card for H<sub>2</sub>O can be written as,

M1 1001.21c -0.1112

8016.21c -0.8888

Here we have taken only <sup>1</sup><sub>1</sub>H and <sup>16</sup><sub>8</sub>O, one can use the remaining isotopes of both elements with consideration of their abundance.

The detector in MCNP is referred as Tally. Any volume, surface or point where the user is interested to calculate flux, current etc., needs to be written after the tally card. There are F1, F2, F4, F5, and F8 are the tallies used in MCNP. The descriptions of these tallies are as below in Table 2.1 [21-23].

**Table 2.1** Details of tally description available in MCNP [21-23]

<b>Mnemonic</b>	<b>Tally Type</b>	<b>Particle pl</b>	<b>Fn Unit</b>	<b>*Fn Unit</b>
F1:pl	Surface current	N or P or N, P or E	-	MeV
F2:pl	Average flux on a surface	N or P or N, P or E	/cm <sup>2</sup>	MeV/cm <sup>2</sup>
F4:pl	Average flux in a cell	N or P or N, P or E	/cm <sup>2</sup>	MeV/cm <sup>2</sup>
FMESH4:pl	Mesh plot for volume average mesh flux in 3D	N or P or E	/cm <sup>2</sup>	MeV/cm <sup>2</sup>
F5a:pl	Flux at a point or ring	N or P	/cm <sup>2</sup>	MeV/cm <sup>2</sup>
FIP5:pl	Pin – hole flux image	N or P	/cm <sup>2</sup>	MeV/cm <sup>2</sup>
FIR5:pl	Planar radiograph flux image	N or P	/cm <sup>2</sup>	MeV/cm <sup>2</sup>
FIC5:pl	Cylindrical radiograph flux image	N or P	/cm <sup>2</sup>	MeV/cm <sup>2</sup>
F6:pl	energy deposition	N or P or N, P	MeV/g	jerks/g
F7:pl	fission energy deposition in a cell	N	MeV/g	jerks/g
F8:pl	pulse height distribution in a cell	P or E or P, E	pulses	MeV

These tallies can be modified with other data cards, e.g., if one is interested to calculate the dose rate in place of the flux, then one has to use DF card with flux to dose conversion factors in the definition of tally F4. There are plenty of



options are available in MCNP, which are discussed in details in MCNP manuals [22, 23].

In present thesis work, the F4 tally and F8 tallies were used with the MCNP – 6.1 version [19]. The tally F4 was used to calculate the average flux inside the target sample, and F8 tally to calculate the detector efficiency which is discussed in Chapter – 5.

## **2.6 Summary**

The different nuclear reaction models were briefly introduced in the present chapter. The brief introduction of TALYS, EMPIRE and MCNP codes were given. The important level density models, which were used in the present thesis work, are listed. Brief idea about the MCNP input file and different blocks necessary for the problem description are discussed.

## References

- [1] N. Bohr, Nature, 137 (1936) 344.
- [2] V. F. Weisskopf and D. H. Ewing, Phys. Rev. 57, 472, 935(1940).
- [3] W. Hauser and H. Feshbach, Phys. Rev. 87, 366(1952).
- [4] J. Griffin, Phys. Lett., 17, 478(1966).
- [5] C. Kalbach-Cline, Nucl. Phys. A210, 590(1973).
- [6] H. Nishioka, et al., Ann. Phys. (NY) 172, 67(1986).
- [7] H. Nishioka, H. A. Weidenmuller and S. Yoshida, Ann. Phys. (NY) 183,166(1988).
- [8] H. A. Bethe, Rev. Mod. Phys. 9, 69(1937).
- [9] A. Koning, S. Hilaire, and S. Goriely, TALYS-1.6 - A Nuclear Reaction Program, User Manual, 1<sup>st</sup> edition (NRG, The Netherlands, 2013).
- [10] M. Herman, et al., EMPIRE-3.2 Malta modular system for nuclear reaction calculations and nuclear data evaluation (2013).
- [11] W. Dilg, W. Schantl, H. Vonach, and M. Uhl, Nucl. Phys. A217, 269 (1973).
- [12] A. V. Ignatyuk, K.K. Istekov, and G. N. Smirenkin, Sov. J. Nucl. Phys. 29, no. 4, 450 (1979).
- [13] A. V. Ignatyuk, J.L. Weil, S. Raman, and S. Kahane, Phys. Rev. C47, 1504 (1993).
- [14] A. D'Arrigo et al., J. Phys. G20, 305 (1994).
- [15] S. Goriely, F. Tondeur, J. M. Pearson, Atom. Data Nucl. Data Tables 77, 311 (2001).
- [16] S. Goriely, S. Hilaire and A. J. Koning, Phys. Rev. C 78, 064307 (2008).
- [17] S. Goriely, M. Samyn, and J. M. Pearson, Phys. Rev. C 75, 064312 (2007).
- [18] R. Capote, et al., Nuclear Data Sheets 110, 3107 (2009).
- [19] Retrieved from: <https://laws.lanl.gov/vhosts/mcnp.lanl.gov/index.shtml>, (24<sup>th</sup> May 24, 2017).
- [20] J. K. Shultis and R. E. Faw, An MCNP Primer (2011).
- [21] T. Goorley, et. al., "Features of MCNP6", Supercomputing in Nuclear Applications and Monte Carlo 2013, Paris, Oct 27-31, LA-UR-13-28114 (2013).

- [22] X-5 Monte Carlo Team, MCNP — A General Monte Carlo N-Particle Transport Code, Version 5, Vol. I (2013).
- [23] X-5 Monte Carlo Team, MCNP — A General Monte Carlo N-Particle Transport Code, Version 5, Vol. II (2013).